Improved Confinement in High-Density Ohmic Discharges in ASDEX

F. X. Söldner, E. R. Müller, F. Wagner, H. S. Bosch, A. Eberhagen, H. U. Fahrbach, G. Fussmann, O. Gehre, K. Gentle,[a] J. Gernhardt, O. Gruber, W. Herrmann, G. Janeschitz, M. Kornherr, K. Krieger, H. M. Mayer, K. McCormick, H. D. Murmann, J. Neuhauser, R. Nolte, W. Poschenrieder, H. Röhr, K.-H. Steuer, U. Stroth, N. Tsois,[b] and H. Verbeek

Max-Planck-Institute für Plasmaphysik, EURATOM Assocation, D-8046 Garching bei Munchen, West Germany

(Received 16 May 1988)

The unsaturated linear rise of the energy confinement time with density, $\tau_E \sim \bar{n}_e$, up to the density limit is recovered in Ohmically heated discharges in ASDEX. Improvement of a factor of 2 is reached with $\tau_E \approx 150$ ms at $\bar{n}_e = 5\times10^{13}$ cm^{-3}. The improved state is characterized by peaked density profiles. The ion heat diffusivity decreases to the neoclassical value. The parameter $\eta_i = L_{n_e}/L_{T_i}$, governing the onset of ion-temperature-gradient modes, falls to the stability threshold. The improvement in confinement might therefore be attributed to the stabilization of η_i modes.

PACS numbers: 52.50.Gj, 52.55.Fa, 52.55.Pi

The scaling of the energy confinement time with density constitutes one of the basic elements in the development of tokamak devices to a fusion reactor. In Ohmic discharges a favorable linear dependence $\tau_E \sim \bar{n}_e$ was first found in Pulsator[1] and Alcator-*A*.[2] In larger machines, however, τ_E saturated at higher density, as observed in Alcator-*C*,[3] D-III,[4] and many other tokamaks.[5] In a few cases of special operation the linear increase of τ_E with $\bar{n}_e$ could be reestablished at high density in otherwise saturated regimes: With pellet injection, the linear confinement regime was greatly extended.[6,7] Optimization of the gas feed reduced the degradation of τ_E.[8] In situations where radiation losses from the plasma edge dominate the power balance, the saturation of τ_E with $\bar{n}_e$ could be overcome by the switching off of the external gas feed.[9] These results suggest that particle refueling plays a crucial role for the confinement behavior. In ASDEX, the modifications of the divertors for the requirement of long pulse heating[10] reduced the gas-pumping surface by an order of magnitude, resulting in an increase of the recycling coefficient. With the reduced gas-puffing rate, superior confinement is now obtained, with the original Alcator-INTOR scaling, i.e., $\tau_E \sim \bar{n}_e$, extended up to the density limit.

In this Letter, the transition from the saturated to the new improved Ohmic confinement (IOC) regime is analyzed. Changes in the particle and energy transport are discussed.

Improved confinement is obtained in stationary deuterium discharges at densities above $\bar{n}_e \approx 3\times10^{13}$ cm^{-3}, the previous τ_E saturation limit. The confinement quality also critically depends on the wall conditions. Improved confinement is achieved with uncoated stainless-steel walls and with carbonized walls conditioned by He-glow discharges for low gas release. Density-rampup shots and hydrogen discharges, both with higher gas consumption, exhibit the usual confinement characteristics with rollover and saturation of τ_E. Access to the improved confinement regime therefore seems to depend essentially on the ratio of neutral-gas fueling to recycling. Similar observations were made in other regimes of improved confinement: With pellet injection, superior confinement is achieved at low levels of additional gas puffing,[7] and the supermode in TFTR requires careful preconditioning of the interior walls for high gas pumping capability.

The transition from the saturated regime to the IOC regime during one discharge is shown in Fig. 1. As the preprogrammed density plateau is being approached, the external gas feed is reduced at 1.17 s by feedback control. With falling gas flux the density profile $n_e(r)$ is continuously peaking, as seen from the ratio V_n of the line-integrated densities measured by HCN interferometry at $r/a = 0.75$ and $r = 0$. Local profile measurements with a Li beam at the plasma edge and laser light scattering over the whole plasma cross section reveal first a drop of density at the edge (at the separatrix, $\Delta n_{es}/n_{es} \approx -0.4$) and, after some delay, a rise of $n_e(0)$. With decreasing separatrix density the electron pressure in the divertor also decreases. The D_α emission in main chamber and divertor drops. Soft x-ray (SX) emission increases and shows a drastic change in the sawtooth behavior. The sawtooth period increases by a factor of about 2 and the amplitude also rises. Electron-cyclotron emission measurements, however, show that the amplitude of the sawteeth on the electron temperature even decreases [$\Delta T_e(0)/\bar{T}_{e0}$, 9% → 6%]. The large sawteeth on the SX radiation therefore seems to be mainly determined by changes in the impurity concentration. Some channels of the SX camera reverse the sawtooth pattern in the time from 1.35 to 1.5 s: The signal at 12.5 cm changes from inverted to normal sawteeth. The same is seen on the symmetric channel on the other side. An expansion of the $q = 1$ surface during this phase therefore has to be concluded, with the sawtooth inversion radius increasing from 11 to 14 cm. This indicates a peaking in

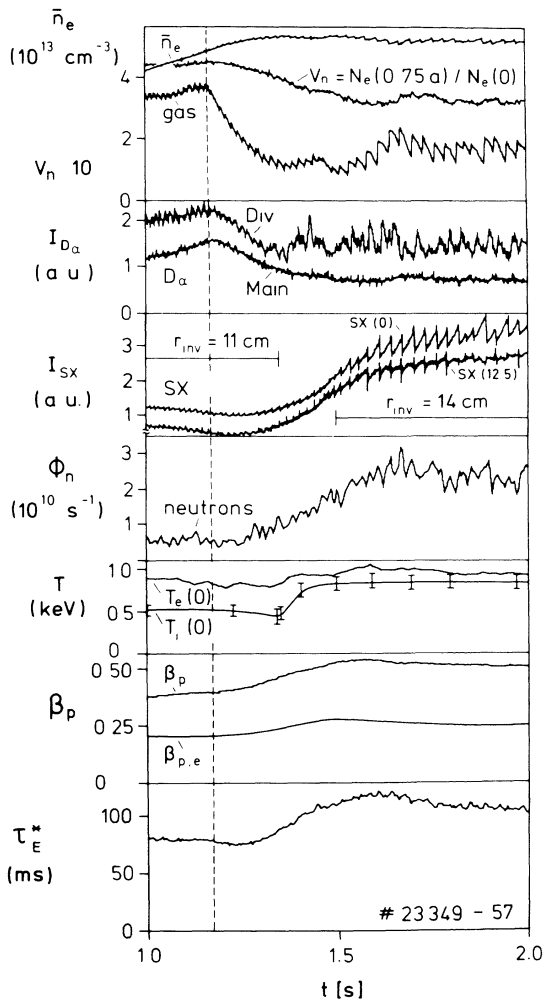

FIG. 1. Temporal evolution of plasma parameters during the transition from the saturated to the extended linear confinement regime. $I_p = 380$ kA, $B_t = 2.17$ T, $q(a) = 2.75$.

the current profile $j(r)$, which is also seen from an increase of l_i as determined from both magnetic measurements and the electron temperature profile with the assumption of neoclassical conductivity. The central electron and ion temperatures increase, with $T_i(0)$ rising essentially during the phase of expansion of the $q = 1$ surface. The poloidal β from magnetic measurements as well as $\beta_{p,e}$ from laser scattering measurements slowly increase. The Ohmic power input slightly decreases by about 15%. The confinement time τ_E^* rises from $\simeq 80$ to $\simeq 125$ ms. During the transition to improved confinement the radiation profile is peaking, while the total radiation losses remain roughly constant.[11]

The transition from the saturated confinement regime at the end of the $\bar{n}_e$ rampup phase to the improved confinement regime during the flat-top phase is smooth, and stationary conditions are attained only after about 0.5 s. The improvement of confinement might therefore be related to the slow profile changes, essentially of

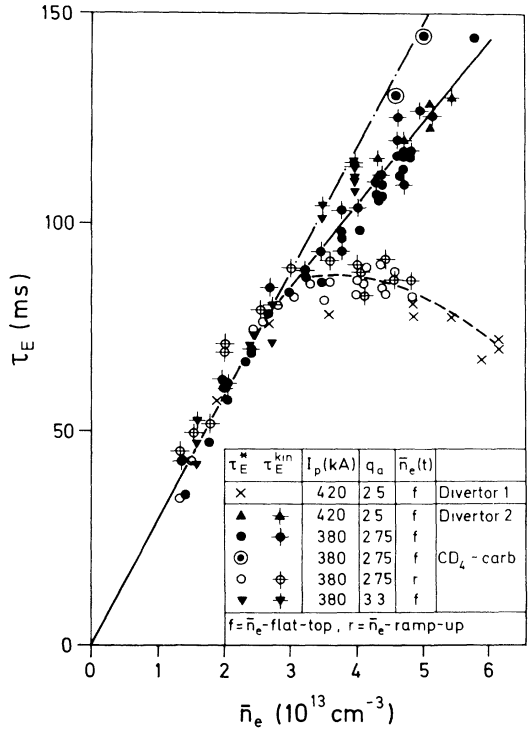

FIG. 2. Scaling of the global energy confinement times τ_E^* (from magnetic measurements) and τ_E (from kinetic measurements) with density.

$n_e(r)$, which occur on the same time scale. The initial trigger, however, seems to be the reduction of the gas flux, leading to an immediate drop of the density at the separatrix. D_α emission and neutral-particle outflux also decrease without delay. An improvement of the particle confinement at the edge has to be concluded from this, which then initiates the peaking of the density profile.

The improved confinement has been obtained for a large range of parameters, with $I_p = 300$–450 kA, $B_t = 2.17$–2.8 T, $q_a = 2.5$–3.5. The scaling of the energy confinement times τ_E^* (from magnetic measurements of β_p) and τ_E [from kinetic measurements of $n_e(r)$, $T_e(r)$, and $T_i(r)$] with density is shown in Fig. 2. Values of up to $\tau_E \approx 150$ ms are obtained at 5×10^{13} cm^{-3} after light CD_4 carbonization and at 5.85×10^{13} cm^{-3} with constant gas flow and slowly rising density $\bar{n}_e$. The points on the saturated branch are obtained from $\bar{n}_e$ rampup shots and from old flat-top deuterium discharges with the large chambers of divertor 1. The dashed-dotted line is extrapolated from the linear regime at low density. The points with special CD_4 carbonization fully recover this scaling at high density.

The shape of the density profile is closely correlated with the distinct confinement regimes. The ratio $Q_n = n_e(0)/\langle n_e \rangle$ is plotted in Fig. 3 for a density scan with $\bar{n}_e$ flat-top and $\bar{n}_e$ rampup discharges. In the saturated confinement regime $n_e(r)$ is always flat with a peakedness factor of ~ 1.45. In the improved extended linear

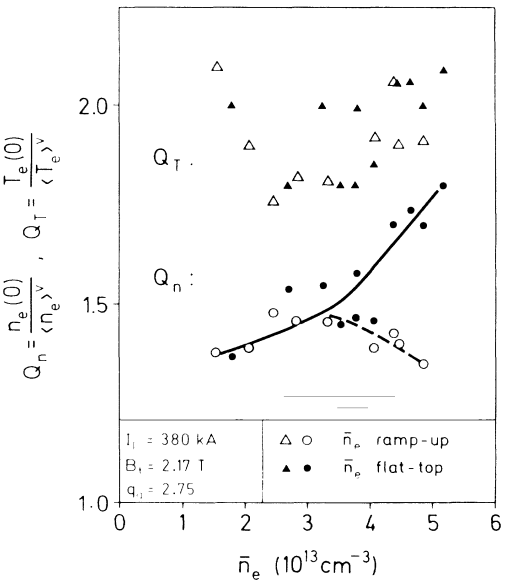

FIG. 3. Scaling of the profile parameters $Q_n = n_{e0}/\langle n_e \rangle$ and $Q_T = T_{e0}/\langle T_e \rangle$ with density.

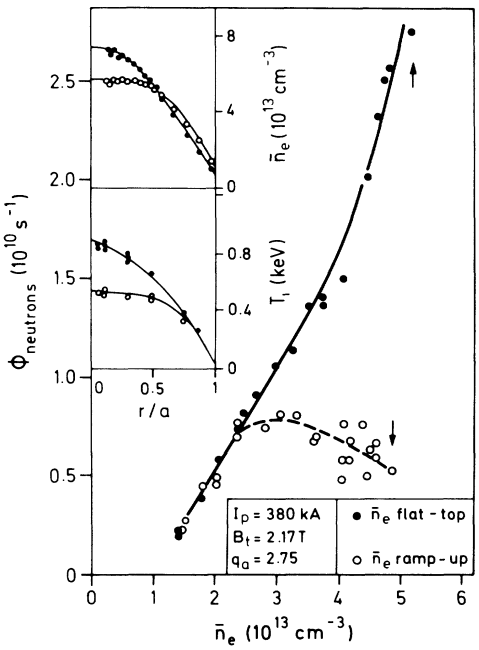

FIG. 4. Variation of the neutron flux with density. Radial profiles of $n_e(r)$ and $T_i(r)$ for the densities marked by arrows.

regime $n_e(r)$ is peaking and Q_n increases with $\bar{n}_e$. For the electron temperature, no systematic variations of the form of the profile are seen.

In the good confinement regime a strong increase of the neutron flux with density is observed, as shown in Fig. 4, resulting from both the increase in the central temperatures and the peaking of the $n_e(r)$ profile.

Transport in the two confinement regimes was studied by various techniques. The particle confinement of ions of the main species increases during transition to the extended linear regime, as seen from the decreases in neutral pressure, D_α emission, and outflux of low-energy neutrals onto the wall. Differences in the particle confinement are seen in experiments in which the gas feed is switched off during the current flat top. The decay time for the plasma density is a factor of 2.5 as long in the good confinement regime. Finally, the local particle transport parameters D_p (diffusion coefficient) and v_{in} (inward drift velocity) were determined from gas oscillation experiments: Small density perturbations are induced in this case by our modulating the external gas feed. Their radial propagation is followed by our solving the particle transport equation with D_p and v_{in} as fitting coefficients.[12] The results are summarized together with other transport parameters in Table I. In the IOC regime the diffusion coefficient drops in the gradient region by an order of magnitude. The inward drift in this region also decreases.

The impurity transport was studied with laser blowoff of Ti. An increase by a factor of 3 of the particle confinement time, from 55 to 185 ms, is determined from the decay times of TiXX. The improved impurity confinement leads to accumulation of intrinsic heavy impurities in the plasma center. The radiation profile then peaks in the center and Z_{eff} increases. In the discharges of Fig. 1, the volume-averaged Z_{eff} rises from 1.9 to 2.3, and the central Z_{eff} obtained from bremsstrahlung increases from 1.7 to 2.5. The influx of light and heavy impurities diminishes at the same time because of reduced particle flux onto the wall and hence reduced sputtering. Transitions to enhanced impurity confinement upon switch off of the external gas feed were also observed on T-10.[13]

TABLE I. Transport parameters.

Transport parameters	Saturated confinement ($t = 1.2$ s)	IOC ($t = 1.8$ s)
	Experiment A[a]	
$\bar{n}_e$ (10^{13} cm^{-3})	4.9	5.2
τ_E^* (ms) $= W_p^*/P_{OH}$	83	112
$\chi_e(2a/3)$ (m^2/s)	0.35	0.28
$\chi_i(2a/3)$ (m^2/s)	$0.7 = 2\chi_{CH}$	$0.4 = \chi_{CH}$
$\eta_e(2a/3)$	1.9	1
$\eta_i(2a/3)$	1.5	1
	Experiment B[b]	
$\bar{n}_e$ (10^{13} cm^{-3})	3	5
τ_p (ms)	55	185
$D_p(2a/3)$ (m^2/s)	0.5	0.06
$v_{in}(2a/3)$ (m/s)	4	1.5

[a]No. 23349-57.
[b]No. 23344-47, 23608, 10.

The energy transport was analyzed with the 1D code TRANSP. There the radial power fluxes are calculated from the measured profiles of density, temperature, and radiation, and heat transport coefficients are derived. In the IOC regime the electron heat diffusivity decreases by about a factor of 2 over the whole plasma cross section. The ion heat diffusivity has to be reduced from $\chi_i = 2\chi_i^{\text{ncl}}$ in the saturated regime to the neoclassical value in order to fit the experimentally measured profiles in the improved confinement regime. The increased anomalous ion heat conduction losses in the saturated regime are often attributed to η_i modes.[14] In fact, in the saturated regime the critical parameter $\eta_i = d\ln T_i/d\ln n_e = L_{n_e}/L_{T_i}$ is above the instability threshold. In the improved confinement regime, however, η_i and also η_e drop to 1, and possibly below the onset threshold. This suggests that the stabilization of η_i modes through the peaking of the density profile might explain the improvement in confinement and the recovery of the linear $\tau_E \sim \bar{n}_e$ scaling. The peaked density profiles can be formed due to the strong reduction in particle transport after the gas feed decreases.

The discovery of the improved Ohmic confinement regime allows the linear scaling $\tau_E \sim \bar{n}_e$ to be extended up to the density limit. The main mechanism providing superior confinement seems to be the peaking of the density profile. This new regime might form, together with pellet injection, neutral-beam counterinjection,[15] and the supermode of TFTR, a common class of plasma states where improvements in confinement closely correlate with peaked density profiles. Transport code calculations for all these regimes show that the resulting stability of η_i modes could be the unique feature responsible for the superior confinement.

---

[a]Permanent address: University of Texas at Austin, Austin, TX 78712.

[b]Permanent address: NRS Demokritos, Attiki, Athens, Greece.

[1]O. Klüber *et al.*, Nucl. Fusion **15**, 1194 (1975).

[2]M. Gaudreau *et al.*, Phys. Rev. Lett. **39**, 1266 (1977).

[3]S. Fairfax *et al.*, in *Proceedings of the Eighth International Conference on Plasma Physics and Controlled Nuclear Fusion Research, Brussels, 1980* (IAEA, Vienna, 1981), Vol. 1, p. 439.

[4]S. Ejima *et al.*, Nucl. Fusion **22**, 1627 (1982).

[5]R. J. Goldston, Plasma Phys. Controlled Fusion **26**, 87 (1984).

[6]M. Greenwald *et al.*, Phys. Rev. Lett. **53**, 352 (1984).

[7]M. Kaufmann *et al.*, Nucl. Fusion **28**, 827 (1988).

[8]S. Sengoku, J. Nucl. Mater. **145–147**, 556 (1987).

[9]R. R. Weynants *et al.*, in *Proceedings of the Fourteenth European Conference on Controlled Fusion and Plasma Physics, Madrid, Spain, 1987,* edited by S. Methfessel (European Physical Society, Switzerland, 1987), Vol. 1, p. 197.

[10]H. Niedermeyer *et al.*, to be published.

[11]E. R. Müller *et al.*, in *Proceedings of the Fifteenth European Conference on Controlled Fusion and Plasma Physics, Dubrovnik, Yugoslavia, 1988* (European Physical Society, Petit-Lancy, Switzerland, 1988), Vol. 1, p. 19.

[12]O. Gehre *et al.*, in Ref. 11, Vol. 1, p. 7.

[13]N. L. Vasin *et al.*, in Ref. 11, Vol. 1, p. 59.

[14]D. L. Brower *et al.*, Phys. Rev. Lett. **59**, 48 (1987).

[15]O. Gehre *et al.*, Phys. Rev. Lett. **60**, 1502 (1988).